

Image Analysis Based on the Discrete Magnetic Field Generated by the Virtual Edge Current in Digital Images

X. D. ZHUANG¹ and N. E. MASTORAKIS^{1,2}

1. WSEAS Research Department,
Agiou Ioannou Theologou 17-23, 15773, Zografou, Athens, GREECE
xzhuang@worldses.org, xzh_wseas@tom.com
2. Department of Computer Science, Military Institutions of University Education,
Hellenic Naval Academy, Terma Hatzikyriakou, 18539, Piraeus, GREECE
mastor@wseas.org <http://www.wseas.org/mastorakis>

Abstract: - In this paper, the spatial property of the magneto-static field generated by the stable current is discussed and exploited in image analysis. The region-division feature of the magnetic field generated by a current element on 2D plane is investigated experimentally for some simple test images. The virtual edge current in gray-scale images is presented by a magneto-static analogy, which is composed of the tangent edge vectors as a discrete form of the physical current element. The virtual magnetic field generated by the edge current in digital images is investigated experimentally, which is applied in region border detection and region division. A novel image segmentation method is proposed based on the virtual magnetic field generated by the edge current. The experimental results prove the effectiveness of the proposed method, and also indicate the promising application of the physics-inspired methods in image processing tasks.

Key-Words: - Image analysis, virtual edge current, magnetic field, tangent edge vector, image segmentation

1 Introduction

Nature inspired methods have become an important way to solve many theoretical and practical problems for human beings, such as the genetic algorithm, ant colony optimization, neural network, etc [1-8]. In signal and image processing, the nature inspired methods have also been studied and applied. In recent years, the physical field inspired methods have attracted more and more research interest, and such research has achieved promising results for image processing tasks [9-18]. Such results have been applied in image segmentation, biometrics, corner detection, etc [9-18]. The view of regarding a digital image as a virtual field imitating the field in physics may obtain a natural way of image structure presentation and decomposition for further analysis, and may reveal novel features useful in practical tasks.

The electro-magnetic field in physics has a complete set of theoretical description (a series of laws and theorems). There are on-going research efforts to explore the practical use of the methods imitating the electro-magnetic rules in signal and image analysis [9-18]. In this paper, the region-dividing feature of stable magnetic fields is analyzed, based on which the tangent edge vector and the virtual edge current are proposed to represent the edge structure of images. The properties of the virtual magnetic field generated by the virtual edge current are investigated, and a novel

method for image segmentation is proposed based on the direction distribution of the virtual magnetic field. The experimental results prove the effectiveness of the proposed method, and indicate the promising application of the virtual edge current in image processing tasks.

2 The Region-Dividing Feature of the Magnetic Field Generated by Stable Currents on 2D Plane

The distinctive feature of physics-inspired methods for image analysis is a kind of natural description and representation of image structures, which may reveal novel image features for further analysis. The magnetic field generated by the stable current satisfies the Biot-Savart law [19,20], and in this paper its spatial property on the 2D plane is investigated. The possible application of the magneto-static field's spatial property to region border extraction is also discussed.

2.1 The magnetic field of the current in a straight wire and its spatial property

According to the electro-magnetic theory, the magnetic field generated by the stable current in an infinitely long straight wire is [19,20]:

$$B = \frac{\mu_0 I}{2\pi r} \quad (1)$$

where B is the magnitude of the magnetic induction at a space point, I is the intensity of the current, r is the distance of the space point to the straight line, μ_0 and π are two constants. The diagram of the magnetic field generated by the straight line is shown in Fig. 1.

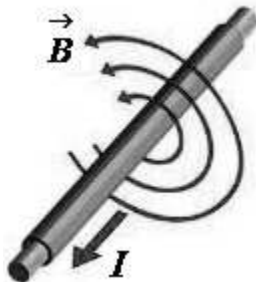


Fig. 1 The magnetic field generated by the straight line

In Fig. 1, the direction of the magnetic induction is determined by the right-hand rule: if the thumb of the right hand is pointed in the direction of the current, and the other four fingers assume a curved position, the magnetic field circling around the wire flows in the direction in which the other four fingers point [19,20]. The right-hand rule is shown in Fig. 2.

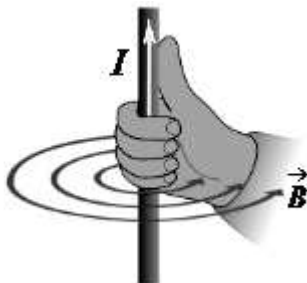


Fig. 2 The right-hand rule

According to the right-hand rule, the direction distribution of \vec{B} can be determined on a plane where the wire lies. Fig. 3 shows the direction distribution of the magnetic field on the 2D plane where the straight wire lies. In Fig. 3 the cross represents the direction of going into the paper, and the dot represents the direction of coming out of the paper. From the viewpoint of geometry, the line divides the plane into two halves. The direction of the magnetic induction vectors in one half is just opposite to that in the other half. If the direction of I is given, based on the direction of \vec{B} , it can be decided on which side of the wire the point lies. Therefore, from the viewpoint of image analysis, the direction of the magnetic field can serve as a feature

which indicates the approximate relative position of a point with respect to the straight wire on the plane.

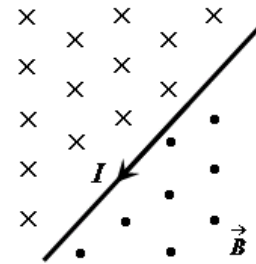


Fig. 3 The direction distribution of the magnetic field generated by a straight wire on a plane

2.2 The magnetic field of the current in a closed wire with arbitrary shape and its spatial property

The straight line is just a special case of curves with arbitrary shapes, and the magnetic field generated by the straight wire is a special case of those generated by general wires. A more general description of the magnetic field is given by the Biot-Savart law [19,20], where the source of the magnetic field is the current of arbitrary shapes which is composed of current elements. A current element $I \vec{dl}$ is a vector representing a very small part of the whole current, whose magnitude is the arithmetic product of I and dl (the length of a small section of the wire). The current element has the same direction as the current flow on the same point. Thus the whole magnetic field is the accumulation of those generated by all the current elements.

The magnetic field generated by a current element $I \vec{dl}$ is as following [19,20]:

$$d\vec{B} = \frac{\mu_0}{4\pi} \cdot \frac{I \vec{dl} \times \vec{r}}{r^3} \quad (2)$$

where $d\vec{B}$ is the magnetic induction vector at a space point, $I \vec{dl}$ is the current element, r is the distance between the space point and the current element, \vec{r} is the vector from the current element to the space point, the operator \times represents the cross product of the two vectors. The direction of the magnetic field also follows the right-hand rule. The magnetic field's direction distribution on the 2D plane where the current element lies is shown in Fig. 4. Similar to the case of straight wire, the direction of the magnetic field reverses when crossing the line on which the current element lies.

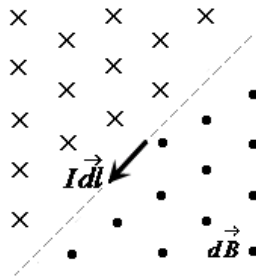


Fig. 4 The magnetic field's direction distribution of a current element on the 2D plane

The magnetic field generated by the current in a wire of arbitrary shape is the accumulation of the magnetic fields generated by all the current elements on the wire, which is described by the Biot-Savart law [19,20]:

$$\vec{B} = \int_D \vec{dB} = \int_D \frac{\mu_0}{4\pi} \cdot \frac{I \, dl \times \vec{r}}{r^3} \quad (3)$$

where \vec{B} is the magnetic induction vector on a space point generated by the whole current elements in a current of arbitrary shape, D is the area where current element exists, \vec{dB} is the magnetic field generated by the current elements in D .

Fig. 5 shows the case of a current element on a closed wire with arbitrary shape, and its magnetic field in the small neighboring area. The closed wire divides the plane into two parts: the inner region and the outer region of the curve. In the small neighboring area of a current element, the magnetic field's direction reverses when crossing the local section of the curve. From the viewpoint of image analysis, the reverse of the field's direction in the local area indicates the existence of the region border (such as the curve in Fig. 5) Therefore, the reverse of the field direction is a promising novel feature representing region borders in digital images, which may be exploited in edge detection and further analysis.

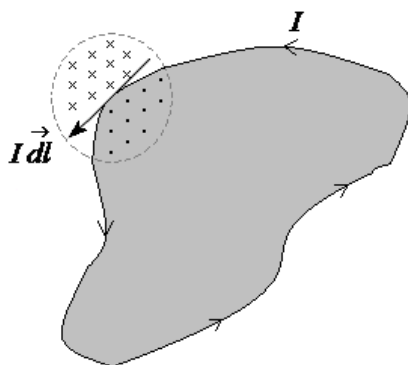


Fig. 5 The magnetic field distribution in the small neighboring area of a current element on a closed wire

3 The Tangent Edge Vector for Simple Image Regions

The direction of the current in a wire is virtually the tangent direction of the curve on that point. On a discrete 2D plane, the discrete form of a current in a curving wire can be represented by a set of tangent vectors on each discrete point of the curve. In geometric theory, for simple regions (such as those in Fig. 4 and Fig. 5) the gradient vector on the region border is perpendicular to the border curve. Since the direction of the curve on a point is represented by the tangent direction of the curve, the tangent vector can thus be estimated by the gradient vector in digital images.

3.1 The definition of the tangent edge vector

In this paper, the tangent edge vector is proposed to represent the edge intensity and direction based on the above sections. The magnitude of a tangent edge vector \vec{T} is defined as the same of the gradient vector \vec{G} on that point, and its direction is perpendicular to the gradient vector:

$$T_x = G_y \quad (4)$$

$$T_y = -G_x \quad (5)$$

where T_x and T_y are the x and y components of \vec{T} respectively, G_x and G_y are the x and y components of \vec{G} respectively. Therefore, the magnitude of the tangent edge vector represents the edge intensity, and its direction represents that of the border curve. Fig. 6 shows the relationship between the gradient and tangent edge vector on the border of a simple region in the image. In this paper, the tangent vector is estimated by rotating the gradient vector clockwise with 90 degrees, which is shown in Fig. 6.

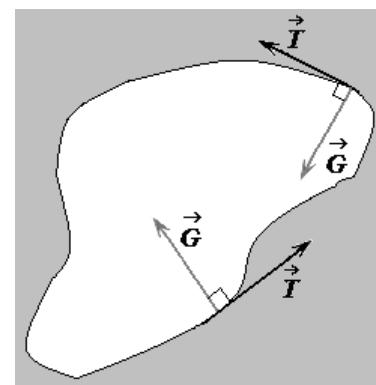


Fig. 6 The relationship between the tangent edge vector and the gradient vector

In this paper, the Sobel operator is adopted to estimate the gradient vector in digital images [21]. The two templates of the Sobel operator for the gradient estimation are shown in Fig. 7.

-1	0	1
-2	0	2
-1	0	1

The template to estimate the gradient component on x-coordinate

1	2	1
0	0	0
-1	-2	-1

The template to estimate the gradient component on y-coordinate

Fig. 7 The two templates of the Sobel operator to estimate the gradient vector

According to the Sobel operator, for digital image $f(x,y)$, the two components of the gradient vector are estimated as following:

$$G_x(x,y)=[f(x+1,y-1)-f(x-1,y-1)]+2[f(x+1,y)-f(x-1,y)]+[f(x+1,y+1)-f(x-1,y+1)] \quad (6)$$

$$G_y(x,y)=-[f(x-1,y+1)-f(x-1,y-1)]-2[f(x,y+1)-f(x,y-1)]-[f(x+1,y+1)-f(x+1,y-1)] \quad (7)$$

where $G_x(x,y)$ and $G_y(x,y)$ are the two components of the gradient vector on the x and y direction respectively. The tangent edge vector can then be estimated based on the gradient vector according to Equation (4) and (5).

3.2 The spatial property of the virtual magnetic field generated by the set of tangent edge vectors

To investigate the properties of the tangent edge vector, some experiments are carried out for a group of simple test images. The original images are shown in Fig. 8(a) to Fig. 12(a) respectively. The test images are with the size of 32×32 , and contain simple image regions. To get a more clear view, the original images are shown in both original size and the size of 4 times larger. The tangent edge vectors are shown in Fig. 8(b) to Fig. 12(b) respectively, where the arrows indicate the directions of the tangent edge vectors and the dot indicates zero vectors.

For the simple test images in the experiments, each region has homogeneous pixels of the same gray-scale. Therefore, the gradient vectors are zero except on the points near the region border. Thus the

tangent edge vectors also gather near the border curve and forms a circulating current around the region as a whole. Therefore, the tangent edge vectors make up a virtual current of a discrete form in the image. Since the physical current elements are along the tangent direction of the wire curve, the tangent edge vector corresponds to the physical current element. The experimental results in Fig. 8(b) to Fig. 12(b) also indicate that the tangent edge vectors form a virtual current in a discrete form along the region border, which is later defined as the virtual edge current in the following section.

To further investigate the tangent edge vector, the virtual magnetic field generated by the tangent edge vectors is calculated. Imitating the physical current element, the discrete virtual magnetic field generated by a tangent edge vector on point (i, j) is proposed as following:

$$\vec{B}_{(i,j)}(x,y) = \frac{\vec{T}(i,j) \times \vec{r}_{(i,j) \rightarrow (x,y)}}{r_{(i,j) \rightarrow (x,y)}^3} \quad (8)$$

where $\vec{B}_{(i,j)}(x,y)$ is the virtual magnetic induction on point (x,y) generated by $\vec{T}(i,j)$, and $\vec{T}(i,j)$ is the tangent edge vector on point (i,j) , $\vec{r}_{(i,j) \rightarrow (x,y)}$ is the vector from (i,j) to (x,y) , and $r_{(i,j) \rightarrow (x,y)}$ is the distance between (i,j) and (x,y) .

Thus the virtual magnetic field generated by all the tangent edge vectors is defined as the accumulation of $\vec{B}_{(i,j)}(x,y)$:

$$\vec{B}(x,y) = \sum_{j=0}^{ROW-1} \sum_{i=0}^{COL-1} \vec{B}_{(i,j)}(x,y) = \sum_{j=0}^{ROW-1} \sum_{i=0}^{COL-1} \frac{\vec{T}(i,j) \times \vec{r}_{(i,j) \rightarrow (x,y)}}{r_{(i,j) \rightarrow (x,y)}^3} \quad (9)$$

where ROW and COL represents the height and width of the digital image respectively. Because each tangent edge vector generates a magnetic field separating the image points on different sides of the local border section, the accumulation of all the virtual magnetic fields generated by all the tangent edge vectors may separate the points into two classes: those within the region and those outside the region. The simulation results are also shown in visible figures. The magnitude of each virtual magnetic field is shown in Fig. 8(c) to Fig. 12(c), where larger gray-scale values represent larger magnitude of $\vec{B}(x,y)$. The direction distribution of each virtual magnetic field is shown in Fig. 8(d) to Fig. 12(d), where the white points represent the direction of going into the paper, and the black points represent the direction of coming out of the

paper. The results indicate that different regions in the image have different directions of the virtual magnetic field, and the field direction reverses when crossing the region orders. Therefore, the direction distribution in the virtual magnetic field can serve as a promising feature for region border detection and also image segmentation.

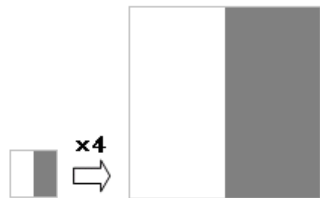


Fig. 8(a) The *test1* image (4 times of original size on the right)

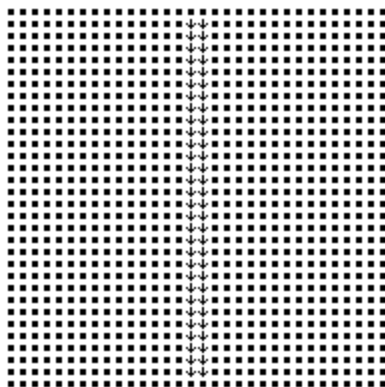


Fig. 8(b) The direction distribution of the tangent edge vectors

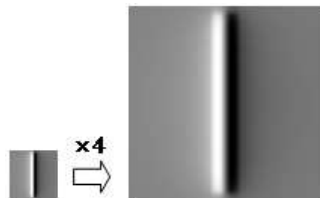


Fig. 8(c) The magnitude distribution of the magnetic field generated by the set of tangent edge vectors (larger gray-scale values represent larger magnitude)

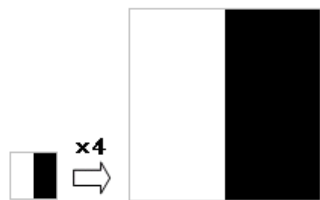


Fig. 8(d) The direction distribution of the magnetic field generated by the set of tangent edge vectors (the white points represent the direction of going into the paper, and the black points represent the opposite direction)

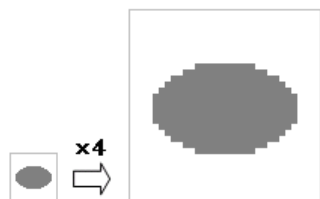


Fig. 9(a) The *test2* image (4 times of original size on the right)

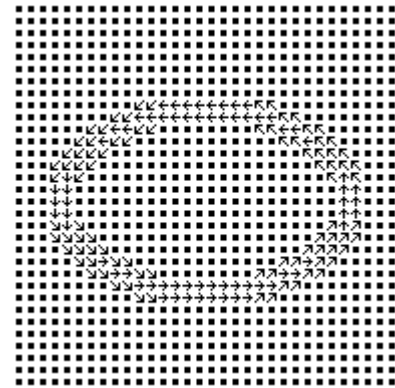


Fig. 9(b) The direction distribution of the tangent edge vectors

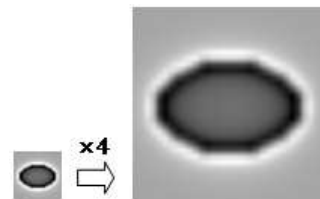


Fig. 9(c) The magnitude distribution of the magnetic field generated by the set of tangent edge vectors (larger gray-scale values represent larger magnitude)

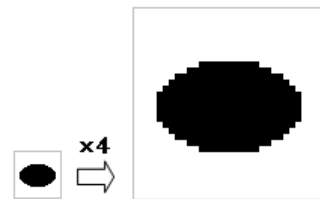


Fig. 9(d) The direction distribution of the magnetic field generated by the set of tangent edge vectors (the white points represent the direction of going into the paper, and the black points represent the opposite direction)

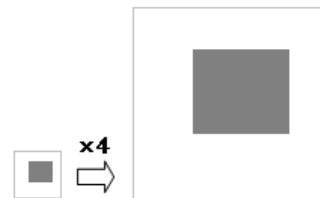


Fig. 10(a) The *test3* image (4 times of original size on the right)

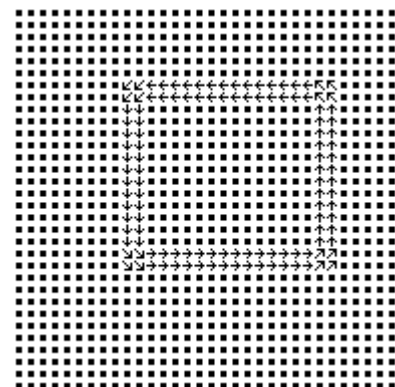


Fig. 10(b) The direction distribution of the tangent edge vectors

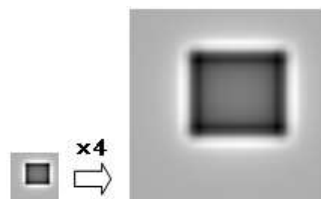


Fig. 10(c) The magnitude distribution of the magnetic field generated by the set of tangent edge vectors (larger gray-scale values represent larger magnitude)

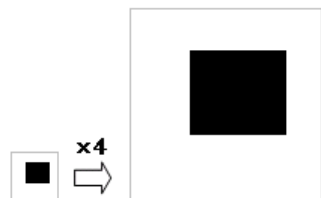


Fig. 10(d) The direction distribution of the magnetic field generated by the set of tangent edge vectors (the white points represent the direction of going into the paper, and the black points represent the opposite direction)

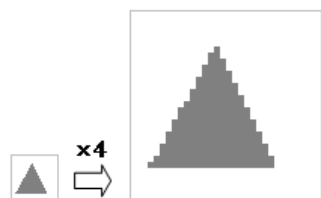


Fig. 11(a) The *test4* image (4 times of original size on the right)

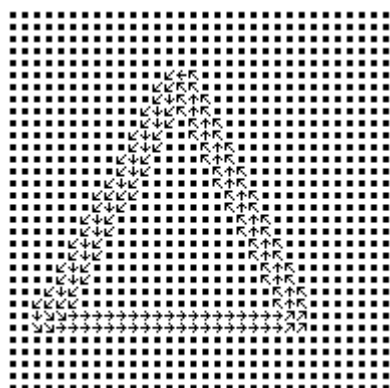


Fig. 11(b) The direction distribution of the tangent edge vectors

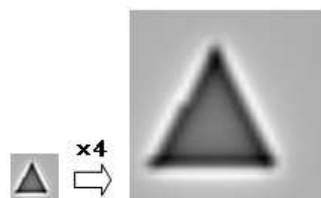


Fig. 11(c) The magnitude distribution of the magnetic field generated by the set of tangent edge vectors (larger gray-scale values represent larger magnitude)

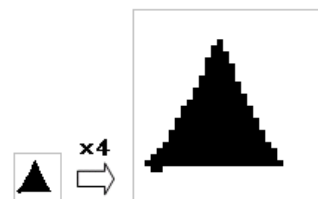


Fig. 11(d) The direction distribution of the magnetic field generated by the set of tangent edge vectors (the white points represent the direction of going into the paper, and the black points represent the opposite direction)

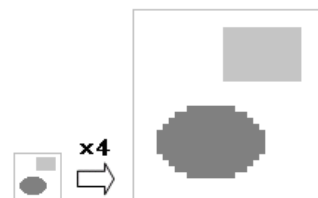


Fig. 12(a) The *test5* image (4 times of original size on the right)

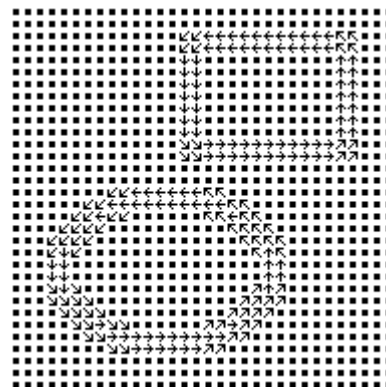


Fig. 12(b) The direction distribution of the tangent edge vectors

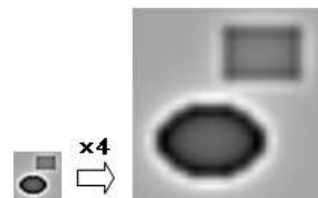


Fig. 12(c) The magnitude distribution of the magnetic field generated by the set of tangent edge vectors (larger gray-scale values represent larger magnitude)

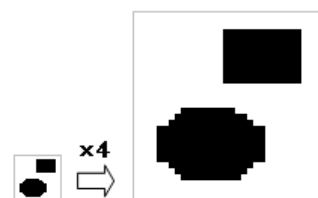


Fig. 12(d) The direction distribution of the magnetic field generated by the set of tangent edge vectors (the white points represent the direction of going into the paper, and the black points represent the opposite direction)

4 The Virtual Edge Current in Digital Images

The images captured in nature (such as photos, satellite images, etc.) have rich gray-scale levels and details, and are much more complex than the simple test images. The digital image can be regarded as a function $f(x,y)$, whose arguments are the position on the 2D plane, and the function value is the gray-scale of the image point [21]. The isolines (contour lines) in the image $f(x,y)$ indicate possible region borders, and in mathematics the gradient vector is perpendicular to the isoline of $f(x,y)$. Consequently, for complex natural images, the tangent edge vector represents the direction of the isoline in the image, i.e. the direction of possible region border curve. On the other hand, since the magnitude of the tangent vector is the same as the gradient vector on that point, its magnitude also indicates the edge intensity on that point. Therefore, the definition of Equation (4) and (5) can also apply to complex natural images. For complex natural images, there may be rich gray-scale levels, and there is a tangent edge vector with some magnitude on each image point. All the tangent edge vectors make up a flow field, and the flow direction on each image point is just the same as that of the tangent edge vector. Therefore, all the tangent edge vectors in a digital image form a virtual current, where the tangent edge vector on an image point serves as the discrete current element. The virtual current composed of the tangent edge vectors as current elements is defined as the virtual edge current, because all the tangent edge vectors are along the direction of the isoline curve in the image.

To investigate the properties of the virtual edge current, the virtual magnetic field generated by the virtual edge current is calculated. Experiments are carried out for a group of natural images. The original images are shown in Fig. 13(a) to Fig. 19(a). The results of the virtual magnetic field are visualized as gray-scale images. The magnitude of each virtual magnetic field is shown in Fig. 13(b) to Fig. 19(b), where larger gray-scale values represent larger magnitude of $\vec{B}(x,y)$. The direction distribution of each virtual magnetic field is shown in Fig. 13(c) to Fig. 19(c), where the white points represent the direction of going into the paper, and the black points represent the direction of coming out of the paper. The experimental results indicate that for natural images the direction of the virtual magnetic field reverses when crossing major region borders. Therefore, the distribution of the virtual

magnetic field can also serve as the basis of border detection and region segmentation.

Because the magnitude of the tangent edge vector is the same as the gradient vector, in

Equation (9) the \vec{T} vectors with large magnitudes have major effect on the formation of overall region borders, while those with small magnitudes can only have effect on adjacent areas and affect the details of the local region borders. In Fig. 13(c) to Fig. 19(c), the experimental results indicate that the region borders can be detected according to the direction distribution of the virtual magnetic field generated by the virtual edge current.



Fig. 13(a) The peppers image



Fig. 13(b) The magnitude distribution of the virtual magnetic field generated by the edge current



Fig. 13(c) The directions distribution of the virtual magnetic field generated by the edge current



Fig. 14(a) The broadcaster image



Fig. 14(b) The magnitude distribution of the virtual magnetic field generated by the edge current



Fig. 14(c) The directions distribution of the virtual magnetic field generated by the edge current



Fig. 15(a) The boat image



Fig. 15(b) The magnitude distribution of the virtual magnetic field generated by the edge current



Fig. 15(c) The directions distribution of the virtual magnetic field generated by the edge current



Fig. 16(a) The cameraman image



Fig. 16(b) The magnitude distribution of the virtual magnetic field generated by the edge current



Fig. 16(c) The directions distribution of the virtual magnetic field generated by the edge current



Fig. 17(a) The house image



Fig. 17(b) The magnitude distribution of the virtual magnetic field generated by the edge current



Fig. 17(c) The directions distribution of the virtual magnetic field generated by the edge current



Fig. 18(a) The medical image of a brain



Fig. 18(b) The magnitude distribution of the virtual magnetic field generated by the edge current



Fig. 18(c) The directions distribution of the virtual magnetic field generated by the edge current



Fig. 19(a) The medical image of a heart



Fig. 19(b) The magnitude distribution of the virtual magnetic field generated by the edge current



Fig. 19(c) The directions distribution of the virtual magnetic field generated by the edge current

5 Image Segmentation Based on the Virtual Edge Current

In the experimental results for the test images, it is shown that the directions of the virtual magnetic field are opposite in two different adjacent regions. This provides a basis of region division in images. In this paper, a method of image region division in the virtual magnetic field generated by the virtual edge current is proposed as following:

- Step1:** Calculate the tangent edge vectors to obtain the virtual edge current;
- Step2:** Calculate the virtual magnetic field generated by the virtual edge current;
- Step3:** Obtain the direction distribution of the virtual magnetic field;
- Step4:** Group the adjacent points with the same direction of virtual magnetic field into connected regions.

The obtained set of connected regions is the result of region division for the gray-scale image.

Real world images consist of more complex region components than the simple test images. To investigate the effect of the above region division method on real world images, experiments are

carried out for a series of real world images. The experimental results are shown from Fig. 20(b) to Fig. 26(b), which are the region division results of Fig. 13(c) to Fig. 19(c) respectively. In Fig. 20(b) to Fig. 26(b), different regions are represented by different gray-scale values. The results indicate that for real world images the region division method may obtain large amount of regions in the image. The numbers of regions obtained for the real world images in the experiments are shown in Table 1.

Table 1

Image	Number of regions
peppers	87
broadcaster	77
boat	149
cameraman	142
house	117
brain	131
heart	342

The region division results of real world images consist of large amount of regions due to the complexity of real world images. To obtain practically useful segmentation result, a region merging method is proposed based on the gray-scale similarity of adjacent regions. First, an expected number of remaining regions after merging is given (usually by trail). Then the following steps are carried out to merge regions until the expected region number is reached:

Step1: For each region in the image, calculate its average gray-scale value.

Step2: Find the pair of neighboring regions with the least difference of the average gray-scale, and merge them into one region.

Step3: If current region number is larger than the expected region number, return to **Step1**; otherwise, end the merging process.

The region merging results for the real world images are shown in Fig. 20(c) to Fig. 26(c), where different regions are represented by different gray-scale. Fig. 20(c) to Fig. 26(c) show the merging results for Fig. 20(b) to Fig. 26(b) respectively.



Fig. 20(a) The peppers image



Fig. 20(b) The region division result based on Fig. 13(c)



Fig. 20(c) The region merging result for Fig. 20(b) (50 regions remained)



Fig. 21(a) The broadcaster image



Fig. 21(b) The region division result based on Fig. 14(c)



Fig. 21(c) The region merging result for Fig. 21(b) (20 regions remained)



Fig. 23(b) The region division result based on Fig. 16(c)



Fig. 22(a) The boat image



Fig. 23(c) The region merging result for Fig. 23(b) (20 regions remained)



Fig. 22(b) The region division result based on Fig. 15(c)



Fig. 24(a) The house image

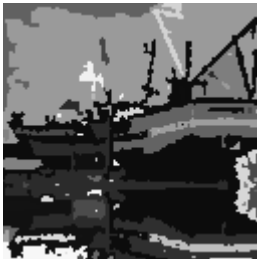


Fig. 22(c) The region merging result for Fig. 22(b) (80 regions remained)



Fig. 24(b) The region division result based on Fig. 17(c)



Fig. 23(a) The cameraman image



Fig. 24(c) The region merging result for Fig. 24(b) (20 regions remained)



Fig. 25(a) The medical image of a brain



Fig. 25(b) The region division result based on Fig. 18(c)

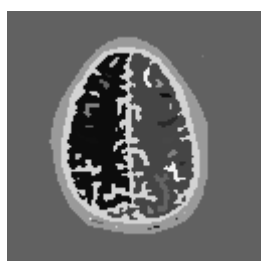


Fig. 25(c) The region merging result for Fig. 25(b) (40 regions remained)

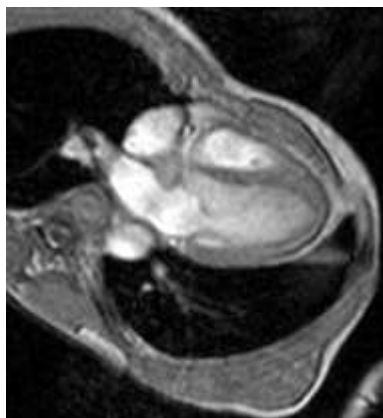


Fig. 26(a) The medical image of a heart

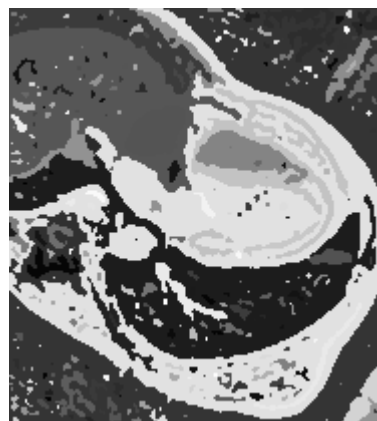


Fig. 26(b) The region division result based on Fig. 19(c)

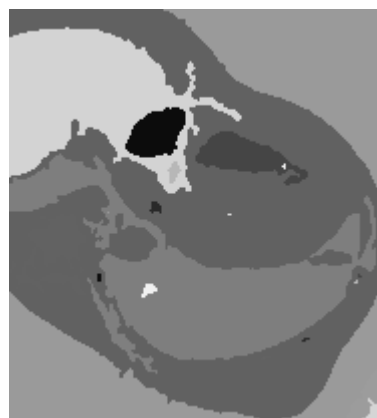


Fig. 26(c) The region merging result for Fig. 26(b) (20 regions remained)

Based on the above sections, in this paper a novel image segmentation method is proposed with the virtual magnetic field generated by the virtual edge current. The procedure of the segmentation is as following:

Step1: Calculate the tangent edge vectors in the image to form the virtual edge current;

Step2: Calculate the virtual magnetic field generated by the virtual edge current;

Step3: Carry out the region division based on the direction distribution of the virtual magnetic field;

Step4: Merge the region division result to a pre-defined number of regions.

The experimental results have proved the effectiveness of the proposed segmentation method.

6 The Influence of Different Edge Intensity Thresholds on Border Formation

The gradient magnitude is the intensity of gray-scale changing at an image point, which is a natural measurement of the possibility of edge existence in the early stage of image analysis. It can be seen from Fig. 13(c) to Fig. 19(c) that the region borders can be determined by the direction distribution of

the virtual magnetic field. In the experimental results, the whole field of $\vec{B}(x, y)$ is formed by the accumulation of all the tangent edge vectors with various magnitudes. Those tangent edge vectors with relatively large magnitudes have major affect on the formation of main region borders. Experiments have been carried out to investigate the effect of different vector magnitude on the formation of region borders. In the experiments, before the calculation of the virtual magnetic field, the tangent edge vectors with magnitudes less than a pre-defined threshold are set to zero, then the virtual magnetic field is formed by the remained vectors with relatively larger magnitudes. In the experiments, the threshold is defined as some percent of the maximum magnitude of the tangent edge vectors. The experimental results for the broadcaster image are shown in Fig. 27(a) to Fig. 27(j). Fig. 27(a) to Fig. 27(e) show the magnitude of the obtained virtual magnetic field, where larger gray-scale values represent larger magnitude of $\vec{B}(x, y)$. Fig. 27(f) to Fig. 27(j) show the direction distribution of the virtual magnetic field, where the white points represent the direction of going into the paper, and the black points represent the direction of coming out of the paper. The threshold values are set as 0%, 0.05%, 0.1%, 0.2% and 0.5% of the maximum gradient magnitude in the image respectively.



Fig. 27(a) The magnitude distribution of the magnetic field generated by the virtual edge current with 0% of the maximum vector length as the threshold



Fig. 27(b) The magnitude distribution of the magnetic field generated by the virtual edge current with 0.05% of the maximum vector length as the threshold



Fig. 27(c) The magnitude distribution of the magnetic field generated by the virtual edge current with 0.1% of the maximum vector length as the threshold



Fig. 27(d) The magnitude distribution of the magnetic field generated by the virtual edge current with 0.2% of the maximum vector length as the threshold



Fig. 27(e) The magnitude distribution of the magnetic field generated by the virtual edge current with 0.5% of the maximum vector length as the threshold



Fig. 27(f) The direction distribution of the magnetic field generated by the virtual edge current with 0% of the maximum vector length as the threshold



Fig. 27(g) The direction distribution of the magnetic field generated by the virtual edge current with 0.05% of the maximum vector length as the threshold



Fig. 27(h) The direction distribution of the magnetic field generated by the virtual edge current with 0.1% of the maximum vector length as the threshold



Fig. 27(i) The direction distribution of the magnetic field generated by the virtual edge current with 0.2% of the maximum vector length as the threshold



Fig. 27(j) The direction distribution of the magnetic field generated by the virtual edge current with 0.5% of the maximum vector length as the threshold

Fig. 27(f) and Fig. 27(g) indicate that the tangent edge vectors of small magnitudes have important effect on local region details, which generates many small region borders in Fig. 27(f) and Fig. 27(g). With the threshold value increasing, small region borders become less. Fig. 27(h) shows a nice balance of border accuracy and the degree of detail. When the threshold becomes too large, there is obvious lost of the border accuracy, which is indicated in Fig. 27(i) and Fig. 27(j). The magnitude threshold for the tangent edge vectors can be adjusted experimentally for different requirement of detail level.

7 Conclusion

The spatial property of the physical magneto-static field generated by stable currents provides a suitable model for region border detection and segmentation. In this paper, the tangent edge vector and the virtual edge current are proposed with a magneto-static

analogy. The virtual edge current is defined to be an orthogonal version of the image gradient field. The direction distribution of the discrete magnetic field generated by the virtual edge current is experimentally proved to be a novel feature for border detection and region division. A new image segmentation method is proposed based on the region division result in the virtual magnetic field. Experimental results also prove the effectiveness of the proposed segmentation method. Further work will investigate the application of the virtual edge current in other image processing tasks.

References:

- [1] John H Holland, *Adaptation in Natural and Artificial Systems*, University of Michigan Press, 1975.
- [2] M. Dorigo, V. Maniezzo, and A. Colomi. Positive feedback as a search strategy. Technical Report 91-016, Dipartimento di Elettronica, Politecnico di Milano, Milan, Italy, 1991.
- [3] M. Dorigo, *Optimization, Learning and Natural Algorithms*, PhD thesis, Politecnico di Milano, Italia, 1992.
- [4] Nikos E. Mastorakis, Genetic Algorithms with Nelder-Mead optimization in the variational methods of boundary value problems, *WSEAS Transactions on Mathematics*, Vol. 8, No. 3, 2009, pp. 107-116.
- [5] Stjepan Picek, Marin Golub, Dealings with problem hardness in genetic algorithms, *WSEAS Transactions on Computers*, Vol. 8, No. 5, 2009, pp. 747-756.
- [6] Cecilia Reis, J. A. Tenreiro MacHado, Crossing genetic and swarm intelligence algorithms to generate logic circuits, *WSEAS Transactions on Computers*, Vol. 8, No. 9, 2009, pp. 1419-1428.
- [7] Mohamed Ettaouil, Youssef Ghanou, Neural architectures optimization and genetic algorithms, *WSEAS Transactions on Computers*, Vol. 8, No. 3, 2009, pp. 526-537.
- [8] Kashif Saleem, Norsheila Fisal, M. Ariff Baharudin, Adel Ali Ahmed, Sharifah Hafizah, Sharifah Kamilah, Ant colony inspired self-optimized routing protocol based on cross layer architecture for wireless sensor networks, *WSEAS Transactions on Communications*, Vol. 9, No. 10, 2010, pp. 669-678.
- [9] D. J. Hurley, M. S. Nixon and J. N. Carter, Force field feature extraction for ear biometrics, *Computer Vision and Image Understanding*, Vol. 98, No. 3, 2005, pp. 491-512.

- [10] X. D. Zhuang and N. E. Mastorakis, The Curling Vector Field Transform of Gray-Scale Images: A Magneto-Static Inspired Approach, *WSEAS Transactions on Computers*, Vol. 7, No. 3, 2008, pp. 147-153.
- [11] G. Abdel-Hamid and Y. H. Yang, Multiscale Skeletonization: An electrostatic field-based approach, *Proc. IEEE Int. Conference on Image Processing*, Vol. 1, 1994, pp. 949-953.
- [12] Luo, B., Cross, A. D. and Hancock, E. R., Corner Detection Via Topographic Analysis of Vector Potential, *Pattern Recognition Letters*, Vol. 20, No. 6, 1999, pp. 635-650.
- [13] Andrew D. J. Cross and Edwin R. Hancock, Scale-space vector field for feature analysis, *Proceedings of the IEEE Computer Society Conference on Computer Vision and Pattern Recognition*, 1997, pp. 738-743.
- [14] K. Wu and M. D. Levine, 3D part segmentation: A new physics-based approach, *Proceedings of the IEEE International symposium on Computer Vision*, 1995, pp. 311-316.
- [15] N. Ahuja and J. H. Chuang, Shape Representation Using a Generalized Potential Field Model, *IEEE Transactions PAMI*, Vol. 19, No. 2, 1997, pp. 169-176.
- [16] T. Grogorishin, G. Abdel-Hamid and Y.H. Yang, Skeletonization: An Electrostatic Field-Based Approach, *Pattern Analysis and Application*, Vol. 1, No. 3, 1996, pp. 163-177.
- [17] X. D. Zhuang, N. E. Mastorakis, The relative potential field as a novel physics-inspired method for image analysis, *WSEAS Transactions on Computers*, Vol. 9, No. 10, 2010, pp. 1086-1097.
- [18] X. D. Zhuang, N. E. Mastorakis, The curl source reverse as a magneto-statics inspired transform for image structure representation, *Proceedings of the 13th WSEAS International Conference on Computers - Held as part of the 13th WSEAS CSCC Multiconference*, 2009, pp. 60-66.
- [19] P. Hammond, *Electromagnetism for Engineers: An Introductory Course*, Oxford University Press, USA, forth edition, 1997.
- [20] I. S. Grant and W. R. Phillips, *Electromagnetism*, John Wiley & Sons, second edition, 1990.
- [21] YuJin Zhang, *Image Engineering: Image Processing (2nd Edition)*, TUP Press, Beijing, China, 2006.